

Manuscript Number:

Title: Investigation of gravity wave activity based on operational
radiosonde data from 13 years (1997-2009): climatology and possible
induced variability

Article Type: Research Paper

Keywords: gravity waves; stratosphere; radiosondes; extratropical cyclone

Corresponding Author: Ms. Ricarda Kramer,

Corresponding Author's Institution: German Aerospace Center

First Author: Ricarda Kramer

Order of Authors: Ricarda Kramer; Sabine Wüst; Michael Bittner

Abstract: Atmospheric gravity waves (GWs) are important for the dynamics of the atmosphere. The analysis of 13 years of routine radiosonde data from Prague (50.01° N, 14.27° E) with temporal highly resolved temperature, pressure and wind measurements is presented in order to derive a climatology of gravity wave activity in the lower stratosphere. An annual cycle with a maximum during winter and a minimum during summer is identified. Gravity wave activity is twice as high during winter as during summer. When analyzing individual years, maxima of gravity wave activity and vertical flux of horizontal momentum often appears together with minima in surface pressure. We speculate therefore that at least parts of the interannual variations of gravity wave activity are due to cyclones. These findings are encouraged by the results of wavelet analysis. They show similar periods in vertical flux of horizontal momentum and pressure variance time series. These features may be attributed to planetary waves.

*Highlights (for review)

- Gravity wave activity (GWA) and momentum fluxes are derived from radiosonde data
- Extratropical cyclone activity is investigated at Prague
- Maxima of GWA and momentum fluxes often appear together with minima of pressure
- Similar periods in momentum flux and pressure variance time series
- They may be attributed with planetary waves and cyclone activity

Investigation of gravity wave activity based on operational radiosonde data from 13 years (1997-2009): climatology and possible induced variability

R. Kramer^{1*}, S. Wüst¹, M. Bittner^{1,2}

1German Aerospace Center (DLR-DFD), 82234 Wessling, Germany

2University of Augsburg, 86135 Augsburg, Germany

** Formerly at University of Augsburg*

Corresponding author: Tel. +49 8153 281246, Ricarda.kramer@dlr.de

Abstract

Atmospheric gravity waves (GWs) are important for the dynamics of the atmosphere. The analysis of 13 years of routine radiosonde data from Prague (50.01° N, 14.27° E) with temporal highly resolved temperature, pressure and wind measurements is presented in order to derive a climatology of gravity wave activity in the lower stratosphere. An annual cycle with a maximum during winter and a minimum during summer is identified. Gravity wave activity is twice as high during winter as during summer. When analyzing individual years, maxima of gravity wave activity and vertical flux of horizontal momentum often appears together with minima in surface pressure. We speculate therefore that at least parts of the interannual variations of gravity wave activity are due to cyclones. These findings are encouraged by the results of wavelet analysis. They show similar periods in vertical flux of horizontal momentum and pressure variance time series. These features may be attributed to planetary waves.

Keywords: Gravity waves, climatology, radiosondes, extratropical cyclone

1. Introduction

It is widely accepted that gravity waves (GWs) play a significant role in the dynamics of the atmosphere as they can transport horizontal momentum and energy even over large distances. These aspects are well addressed by a multitude of publications within the past decades (see, for example, Hines, 1960; Lindzen and Holton, 1968; Fritts and Alexander 2003). Very often, GWs are to be handled as so-called subgrid-scale processes and are therefore mainly

represented via parameterizations in both numerical climate and weather-forecast models (e.g. Manzini and McFarlane, 1998; Choi and Chun, 2011; Orr et al. 2010; Stevens et al., 2013). These models frequently turned out to being considerably sensitive to such parameterizations (e.g. Alexander et al., 2010). Therefore, there is an ongoing need to improve them.

Among topographic generation, shear generation and geostrophic adjustment as well as convective systems are known as prominent tropospheric sources of GWs (Holton, 1983; Fritts and Alexander, 2003). Primarily, orographically excited GWs are usually implemented into models (e.g. McFarlane, 1987; Kim and Arakawa, 1995. McFarlane (1987) presented the results of introducing a simple wave drag parameterization into the Canadian Climate Center general circulation model. A new approach to overcome the deficiency of the model to properly treat the enhancement of drag due to low-level wave breaking by including additional statistical information on subgrid-scale orography in the input of the parameterization was presented by Kim and Arakawa (1995). Further investigations were made by Pulido et al. (2012). They developed an inverse technique using data assimilation principles to estimate gravity wave parameters. By defining a cost function that measures the difference between unresolved drag inferred from observations and the gravity wave drag (GWD) calculated with a parameterization scheme, they provided a robust parameter estimation over a broad range of prescribed parameters. This parameterization agrees better with the observed GWD at high latitudes, if the parameters are allowed to vary with latitude. However, the agreement is either good at the upper or at the lower part of the profile (up to 10 hPa). Orr et al. (2010) investigated how a non-orographic GWD parameterization improves middle atmosphere climate and forecasts of the ECMWF (European Centre for Medium-Range Weather Forecasts) model. The implementation into the model replacing Rayleigh friction leads to a more realistic parameterized gravity wave drag and horizontal distribution of momentum flux in the stratosphere. Choi and Chun (2011) studied the convective source and momentum flux spectra of a parameterization of convective gravity wave drag (GWDC) in a three-dimensional spectral space using mesoscale numerical simulations for various ideal and real convective storms. The authors determined two parameters, namely the moving speed of the convective source and the wave propagation direction. These parameters were included in the GWDC parameterization by Song et al. (2005).

GWs are observed by means of several techniques, implying that each measuring technique has its special limitations on GW parameters like wavelength. As global gravity wave characteristics depending on time, height and geographical location are needed for model

input parameters, satellite-based measurements are very useful. Besides satellites (e.g., Preusse et al., 2002; Ern et al., 2004) other measurement techniques include rocketsondes (e.g., Hirota and Niki, 1985; Hamilton, 1991; Eckermann et al., 1994; Wüst and Bittner, 2006), lidar and radar observations (e.g., Sato, 1994; Mitchell et al., 1994; Sato et al., 1997; Riggan et al., 1997; Li et al., 2010), aircraft (e.g., Nastrom et al., 1987; Dörnbrack et al., 2002; Doyle et al., 2002) and radiosondes (e.g., see Vincent et al., 1997; Yoshiki and Sato, 2000; Wang and Geller, 2003; Gong et al., 2008, Zhang et al. 2014, Kramer et al., 2015). Moreover, it is possible to derive gravity wave characteristics in the upper mesosphere from airglow observations (Hines and Tarasick, 1987; Swenson et al., 2000; Bittner et al., 2002; Schmidt et al., 2013). Radiosonde data has proven to be suitable for the study of gravity waves in the troposphere and lower stratosphere. Meteorological institutions and national weather services are releasing radiosondes in a regular manner (for synoptic purposes) providing also information on gravity wave activity in the lower atmosphere from a multitude of sites worldwide. Hamilton and Vincent (1995) demonstrated the advantage of the vertically high resolved measurements of meteorological parameters such like temperature, pressure, humidity and wind. Detailed gravity wave studies based on such data provide valuable statistical information on the seasonal and spatial variability of gravity waves and their sources, propagation and dissipation (see also e.g. Allen and Vincent 1995; Wang and Geller 2003; Moffat-Griffin et al., 2011).

As mentioned above, convection due to cyclones is a prominent gravity wave source. Studies on their effectivity in terms of GW excitation including the estimation of GW parameters (wavelengths, phase speeds, propagation directions) in all atmospheric height-layers are needed. This holds especially in the context of predicting changes of storm/cyclone intensity (Graham and Diaz, 2001; Ulbrich et al., 2007; Kramer et al., 2015) possibly going along with changing cyclone induced GW activity. Additionally, studies about improvements in operational tropical cyclone track forecasts (e.g. Abernethy, 2003; Jung et al., 2011) and operational numerical weather forecast (e.g. Boybeyi et al., 2002; Irvine et al., 2011) request such studies.

The focus of this work is on characterizing GW activity due to cyclone activity at Prague on the basis of 13 years of routine radiosonde measurements. The paper is organized as follows. In section 2 the radiosonde data set used is described in detail, whereas section 3 gives a short introduction on techniques applied for data processing and estimation of gravity wave parameters. Section 4 is devoted to the discussion of the results. In section 5 main results are summarized and concluding remarks are given.

2. Data

The Czech Hydrometeorological Institut (CHMI) performs four operational radiosonde launches each day at 0, 6, 12 and 18 UTC at Prague (50.01° N, 14.45° E). Analysis of this work is based on a 13-year time series (1997-2009) of these routine radiosonde measurements, which include 17523 releases. Most radiosonde releases are performed using Vaisala RS92-KL radiosondes, but different types of balloons (Cosmoprene KKS800, TOTEX TA1000, TOTEX TX800, and TOTEX TA800).

Temperature, pressure and humidity data are available with an accuracy of about 0.5 K, 0.6-1 hPa and 5% relative humidity. An accuracy of less than 0.2 m/s for the wind speed is given for the Vaisala RS92-SGP radiosonde. It is 0.7 m/s for Vaisala RS92-KL. Data are sampled every 5 s during a balloon ascent and the vertical velocity of the balloon accounts for about 5 m/s; this results in a vertical resolution of about 25 m. The radiosondes typically reach altitudes of 25–35 km (see Figure 1). Radiosondes which do not reach at least 25 km height are discarded from further analysis (1402 radiosonde launches are therefore excluded). Investigations of how many profiles of the whole period depending on month have to be discarded, show that January, November and December have the biggest numbers. In 1997 the biggest percentage of yearly released radiosondes did not reach the 25 km level. Also the following years (1998-2002) exhibit much more exclusions than the rest (2003-2009). Note that the maximum altitude the radiosondes reached reveals an annual cycle (see Figure 1). The highest altitudes are reached during the summer period, while balloons burst at lower altitudes during winter. Beside this annual variation of the maximum ascent heights, the peak heights decrease until about 2004. This effect might be at least partially due to several changes in balloon size and type (personal communication with P. Skrivankova, CHMI) during that period. Another aspect could be stratospheric cooling due to climate change (see e.g. Thompson et al., 2011). Balloons burst earlier at low temperatures. This feature is not relevant for our study and will therefore not be regarded here. Since 2004 the annual cycle of maximum heights is almost the same for every year.

3. Methods

GW induced fluctuations are separated from every individual radiosonde profile. A linear superposition principle of GW perturbations for temperature, zonal and meridional wind (T' , u' and v') on a background structure (\bar{T} , \bar{u} and \bar{v}) is assumed: $T = \bar{T} + T'$ (e.g., Pfenninger et al., 1999; Zhang et al., 2012). A sophisticated cubic spline method is used (Bittner et al., 1994). Vertical resolution of filtered data is 100 m; the cut-off wavelength of the low-pass

filter is chosen to be 7 km. This limit is used in order to focus only on mesoscale perturbations and to exclude large-scale circulation patterns such as planetary waves. A typical example for a filtered temperature profile is given in Figure 2. Subtracting the estimated background from the measured profile provides the perturbations: $(u', v', T') = (u, v, T) - (\bar{u}, \bar{v}, \bar{T})$. The quality of detrending is most important for this study, because all additional analyses are based on it. We therefore extensively tested the detrending technique in order to identify/quantify weaknesses. An altitude depending uncertainty in reproducing the background wind and temperature profiles as well as the corresponding perturbations is quantified (see Figure A1 in the Appendix). The cubic spline method used allows representing temperature fluctuations with a mean precision of ± 0.4 K and wind fluctuations with ± 0.5 m/s. As the mean temperature and wind uncertainties due to the filtering are lower than the errors of the radiosonde measurements itself (± 0.5 K and 0.7 m/s, respectively), the detrending method is of sufficient quality for our study and we assume a mean error of 0.5 K and 0.7 m/s for temperature and wind data, respectively. Details concerning the test of the detrending technique are given in the Appendix.

In order to derive a measure for gravity wave activity (GWA) in the altitude regime of 17-25 km, the temperature fluctuations (T') are squared and summed up:

$$\sum_i T'(i)^2 \quad \text{with } i = 17.0, 17.1, \dots, 24.9, 25.0 \text{ km.}$$

The lower height limit is chosen to be 17 km in order to avoid the relatively very sharp temperature minimum at the tropopause, which is difficult to handle with the spline method. The upper height limit is a consequence of the number of radiosondes which reached the stratosphere before the balloon bursts. Moreover, within this atmospheric height segment the buoyancy frequency is relatively constant. This altitude range was studied also in earlier work such as Allen and Vincent (1995), who used the height range of 17 to 24 km or Wang and Geller (2003), who used 18 to 24.9 km. In our work, we focused on height depending GWA by choosing three altitude intervals, namely 15-28 km, 15-30 km, and 17-25 km. It is found that GWA remains almost the same for these height ranges. Figure 3 shows a typical example (year 1998) of the GWA in these three studied height intervals. All three time series are normalized on their maxima to highlight, that the strongest gravity wave signatures are found in all altitude regimes. Therefore, we defined the altitude interval used for the following studies from 17 to 25 km altitude.

In order to investigate middle atmosphere dynamics, vertical flux of horizontal momentum is a prominent measure. The radiosonde measurement technique allows estimating the vertical flux of horizontal momentum of the measured waves by retrieving temperature amplitude and

vertical wavelengths of individual monochromatic gravity waves. For a detailed description of the derivation of the vertical flux of horizontal momentum are derived from radiosonde data, see Kramer et al. (2015).

4. Results and Discussion

In this section results on temporal variability of GWA and gravity wave vertical fluxes of horizontal momentum are presented. The proxy for gravity wave activity in the lower stratosphere is calculated for the whole analysis period. Figure 4 shows three years (2003-2005) of the GWA time series for Prague (solid line). Gravity wave activity varies between $(5 \pm 2) \text{ K}^2$ and $(800 \pm 28) \text{ K}^2$. During all years a basic activity of gravity waves in the lower stratosphere is found, which can be presumably ascribed to a continuous excitation of gravity waves due to orographic sources (Prague is located in the center of the Czech Republic close to several mountains) or to the jetstream. Beside this, enhanced values are observed regularly during winter time (see red boxes). This behavior is confirmed calculating the mean GWA of all years (see Figure 5). Moreover, the seasonality of the mean GWA was analyzed by means of a harmonic analysis (for details see Bittner et al., 1994 and Wüst and Bittner, 2008). Three main periods around ~ 1 year, $\sim 1/2$ year and $\sim 1/3$ year were identified. They are combined and marked by the gray line in Figure 5. Dashed vertical lines denote the approximate transitions from winter to summer period and vice versa.

Besides the mean gravity wave activity of around $(78 \pm 9) \text{ K}^2$, a distinction between summer and winter period shows that winterly gravity wave activity is considerably enhanced by a factor of two compared to gravity wave activity in summer for the studied altitude interval (17-25 km). A likely explanation for the seasonal cycle is critical-level filtering of gravity waves in the seasonally varying background winds (Fukao, 2007). Furthermore, Allen and Vincent (1995) proposed winter storm fronts as a seasonally varying source responsible for the seasonal cycle in wave activity in midlatitude radiosonde observations. Various other studies on gravity wave variances at mid to high latitudes throughout the stratosphere also show an annual cycle with a maximum in winter and a minimum in summer (see Kitamura and Hirota, 1989; Yoshiki and Sato, 2000; Wang and Geller, 2003). A simple linear model, described by Eckermann (1995), explained the annual cycle in lidar and rocket sounding observations without any seasonal variation in gravity wave sources. Following these results larger variances in winter are caused by the fact that the colder winter stratosphere (with correspondingly smaller scale-height and faster decrease in density) leads to faster amplitude growth with height.

Beside orography also convection is a prominent gravity wave source which is usually mentioned when investigating tropical regions (e.g. Karoly et al., 1996; Dutta et al., 2009). However, pressure systems can lead to convection-induced gravity wave generation, also in mid-latitudes (Schneider, 1990; Lehmann et al., 2012; Plougonven and Zhang, 2014; Kramer et al., 2015). In order to analyze to which extent pressure systems can explain the wintery peaks of GWA, Figure 4 shows also the meteorological parameter surface pressure (dashed-dotted line). It is obvious that especially low surface pressure often occurs in conjunction with enhanced GWA (see especially black boxes in Figure 4). However, this correlation appears to be time-shifted (between 6 and 18 hours) in several cases. This may be explained by the excitation direction of GWs, which travel away from their source and therefore reach stratospheric heights over Prague before the center of the cyclone does. Furthermore, the correlation cannot be observed for each peak in the GWA or each decrease in pressure.

In order to have a closer look on the pressure time series Figure 6 shows a typical example of negative values of the surface pressure difference after 12 hours ($\Delta p = p_2 - p_1$, whereby Δp is correlated to GWA_2) of observation (dashed line, lower panel) which are opposed to the corresponding times series of GWA (solid line, upper panel). Gray lines are included to guide the eye. It needs to that the overall consensus of both time series is anti-correlated. Most times enhanced GWA appears 6-18 hours before pressure decreases (a correlation factor of - 0.31 is calculated if pressure decrease values are time shifted by 12 hours). It shall be noted that not every minimum in the pressure time series is related to a low pressure system which is centered over Prague. This implicitly means that the station is influenced by the cyclone even if the cyclone's center is not directly above the station. For midlatitude synoptic scale disturbances like extratropical cyclones the Coriolis force and the pressure gradient force are in approximate balance (geostrophic approximation). Then the geostrophic wind is defined, which approximates the true horizontal velocity to within 10-15 % in midlatitudes (Holton, 2004). We speculate, that depending on its deviation to the center a pressure system influences the zonal wind regime to a different extent and imposes an additional spatially varying gravity wave filter.

As the center of a cyclone is not easy to be localized automatically, each strong pressure decrease, which combined with a GWA peak within a time interval of 12 hours was analyzed by hand using weather maps of the UK Met Office. As mentioned above we found that not every strong pressure decrease is going along with a cyclone centered over Prague, but each pressure decrease corresponds to a low pressure system in the vicinity of the station (~200 km).

As our proxy for GWA is rather simple we calculated the gravity wave vertical flux of horizontal momentum for the zonal and meridional component, respectively, and integrated it over the stratospheric height segment between 17 and 25 km altitude. They range between $(0.3 \pm 0.1) \text{ m}^2/\text{s}^2$ to $(13 \pm 3) \text{ m}^2/\text{s}^2$. These two parameters are shown in Figure 7 (black solid lines) combined with the surface pressure at Prague (dashed line). Obviously, momentum fluxes and surface pressure are in a better correlation than gravity wave activity and surface pressure; note that a clear linear relation is not given, either. Alexander and Holton (1997) showed with their simulation of several squall line cases in the tropics generating gravity waves, that high-frequency gravity waves are dominant in the stratosphere and contribute about one fourth of the total momentum flux forcing the QBO in the tropical stratosphere. Moreover, higher intrinsic frequency gravity waves carry more energy and momentum flux than lower-frequency waves of the same wave energies (Fritts and Vincent, 1987). As radiosondes ascend relatively fast with about 5 to 7 m/s they are sensitive especially to high-frequency GWs. It therefore appears plausible that the time series of vertical fluxes of horizontal momentum at Prague reveals a better correlation than the pressure time series.

Using a wavelet analyses based on Morlet-mother-wavelet, momentum flux and ground pressure fluctuations were analyzed in order to find similar periods in both time series, which yield the correlation between both parameters. Figure 8 shows time series and the contour plots of the relative wavelet intensities of momentum flux (a) and pressure (b) variances due to periods between 12 and 600 hours between 1st January 1998 and 31st March 1998. White lines denote the 95% confidence limit based on a conservative Monte-Carlo method (see Höppner and Bittner, 2007 for deriving the confidence limit). High spectral intensities are connected with periods around 360 hours corresponding to about 15 days in both time series in the upper part of the wavelet analysis. These intensities are due to periodic deep pressure values and high momentum fluxes. The lower part of the wavelet analysis is focused on periods lower than 240 hours. Especially periods of about 120-168 hours (5-7 days) are prominent. Both periods are often observed and they are usually referred to planetary waves (e.g. Forbes, 1995). Planetary waves are linked to high and low pressure systems. Although the wavelet spectrograms do not exactly match always the overall patterns are obviously quite similar. Investigating all the years (1997-2009) other periods (e.g. the 10-day oscillation), which are usually also associated with planetary waves, are found (results are not shown here). Overall, the variability of the vertical fluxes of horizontal momentum at Prague correlates quite well with the variability of the pressure time series and therefore suggests that these parameters are coupled.

Obviously, the GW signatures (represented by momentum fluxes) in the 17-25 km altitude interval are pronounced during cyclone activities. We tentatively interpreted this finding in terms of a non-uniform GW radiation in each direction. This is in accordance with modeling studies (Piani et al., 2000; Alexander et al., 2004; Lehman et al., 2012).

5. Summary and conclusions

13 years (1997-2009) of high vertical resolution radiosonde data from the Czech meteorological station at Prague have been analyzed for gravity wave activity in the lower stratosphere (17-25 km). A cubic spline method was used to separate gravity wave signatures with vertical wavelengths of 7 km and less from gravity waves with longer vertical wavelengths and the background. The sum of squared residuals over the whole height-range was calculated based on temperature data and served as a proxy for gravity wave activity (GWA); additionally vertical fluxes of horizontal momentum were derived from the data.

- Gravity wave activity in the lower stratosphere (17-25 km) over Prague is characterized by an annual cycle with its maximum during winter and its minimum during summer. Winterly gravity wave activity is enhanced by a factor of two compared to gravity wave activity in summer (Fig. 5).

Gravity wave activity and gravity wave induced vertical fluxes of horizontal momentum show variations in the range of around $(5 \pm 2) \text{ K}^2$ and $(800 \pm 28) \text{ K}^2$ and $(0.3 \pm 0.1) \text{ m}^2/\text{s}^2$ to $(13 \pm 3) \text{ m}^2/\text{s}^2$, respectively; the maxima are enhanced by a factor of 10 / 8 compared to background gravity wave activity $(78 \pm 8 \text{ K}^2)$ / total momentum fluxes $(1.7 \pm 1.2 \text{ m}^2/\text{s}^2)$. Similar variations can also be observed in the time series of surface pressure.

- Maxima of gravity wave activity and total momentum fluxes often appear together with minima of surface pressure (Figs. 6, 7).
- Wavelet analysis showed similar periods in vertical flux of horizontal momentum and pressure variance time series. Typical periodicities found are 15d and 10d. These features may be attributed with planetary waves (Fig. 8). It is thus speculated, that at least parts of the GWA is due to cyclone activity.

Appendix: Simulation and test of detrending method

In order to investigate how reliable the detrending method is, 1208 different temperatures as well as wind profiles including gravity wave fluctuations were simulated for a height range of 0-29.7 km. All these synthetic profiles are based on realistic background profiles from radiosonde data and are combined with three different simulated oscillations. These simulated oscillations are generated with a set of parameters: five different starting amplitudes (0.5 K, 1.0 K, ... , 2.5 K), 13 different wavelengths (1.0 km, 1.5 km, ..., 7 km) and eight different phases ($\pi/8, \pi/7, \dots, \pi$). Moreover, five different values are used to increase the amplitudes linear with height (0.05, 0.01, ..., 0.25). From all these 2600 different synthetic oscillations five different ones are selected by a random generator and added to one background profile. After calculating the synthetic profiles, they were detrended. A cubic spline, which is sensitive to vertical wavelengths of 7 km and longer is fitted to and subtracted from each data series. The lower limit of the filtering process is chosen to be 200 m, due to the Nyquist-frequency (data points have an interspace of 100 m). Figure A1 shows the mean uncertainty of the filtering technique applied depending on height for all 1208 temperature as well as wind profiles. The shaded areas mark all values which are lower than the uncertainty of the radiosonde measurements itself. Therefore, the cubic spline method used allows representing temperature fluctuations with a mean precision of +/- 0.4 K and wind fluctuations with +/- 0.5 m/s.

Acknowledgement

The authors thank the Bavarian State Ministry of the Environment and Public Health for funding the project CESAR (Az: U8729-2009/114-18-ZKL01Abt7_18459). We also thank the Czech Hydrometeorological Institute for providing the radiosonde data.

References:

Aberson, S. D., 2003. Targeted Observations to Improve Operational Tropical Cyclone Track Forecast Guidance, *Mon. Weather Rev.*, 131, 1613-1628.

Alexander, M. J., Geller, M., McLandress, C., Polavarapu, S., Preusse, P., Sassi, F., Sato, K., Eckermann, S., Ern, M., Hertzog, A., Kawatani, Y., Pulido, M., Shaw, T. A., Sigmond, M., Vincent, R., Watanabe, S., 2010. Recent developments in gravity-wave effects in climate models and global distribution of gravity-wave momentum flux from observations and models, *Q. J. R. Meteor. Soc.*, 136:1103-1124.

Alexander, M. J., Holton, J. R., 1997. A Model Study of Zonal Forcing in the Equatorial Stratosphere by Convectively Induced Gravity Waves, *J. Atmos. Sci.*, 54, 408-419.

Alexander, M. J., May, P., Beres, J. H., 2004. Gravity waves generated by convection in the Darwin area during Darwin Are Wave Experiment, *J. Geophys. Res.*, 109, D20S04, doi:10.1029/2004JD004729.

Allen, S. J., Vincent, R. A., 1995. Gravity wave activity in the lower atmosphere: Seasonal and latitudinal variations, *J. Geophys. Res.*, 100, 1327-1350.

Bittner, M., Offermann, D., Graef, H.-H., Donner, M., Hamilton, K., 2002. An 18-year time series of OH rotational temperatures and middle atmosphere decadal variations, *J. Atmos. Sol. Terr. Phys.*, 64, 1147-1166.

Bittner, M., Offerman, D., Bugaeva, I. V., Kokin, G. A., Koshelkov, J. P., Krivolutsky, A., Tarasenko, D. A., Gil-Ojedda, M., Hauchcorne, A., Luebken, F.-J., de la Modena, B. A., Mourier, A., Nakane, H., Oyama, K. I., Schmidlin, F. J., Soule, I., Thomas, L., Tsuda, T., 1994. Long period/ large scale oscillations of temperature during the DYANA campaign, *J. Atmos. Terr. Phys.*, 56, 1675-1700.

Boybeyi, Z., Bacon, D. P., Kaplan, M. L., 2002. The use of adaptive (targeted) observations in operational numerical weather forecasting, Pecora 15/Land Satellite Information IV/ISPRS Commission I/FIEOS 2002 Conference Proceedings.

Choi, H.-Y., Chun, H.-Y., 2011. Momentum Flux Spectrum of Convective Gravity Waves. Part I: An Update of a Parameterization Using Mesoscale Simulations, *J. Atmos. Sci.*, 68, 739-759.

Dörnbrack, A., Birner, T., Fix, A., Flentje, H., Meister, A., Schmid, H., Browell, E., Mahoney, M., 2002. Evidence for inertia gravity waves forming polar stratospheric clouds over Scandinavia, *J. Geophys. Res.*, 107, D20, doi:10.1029/2001JD000452.

Doyle, J., Volkert, H., Dörnbrack, A., Hoinka, K., Hogan, T., 2002. Aircraft measurements and numerical simulations of mountain waves over the central Alps: A pre-MAP test case, *Q. J. R. Meteorol. Soc.*, 128, 2175–2184.

Dutta, G., Kumar, M. C. A., Kumar, P. V., Ratnam, M. V., Chandrashekar, M., Shibagaki, Y., Salauddin, M., Basha, H. A., 2009. Characteristics of high-frequency gravity waves generated by tropical deep convection: Case studies. In: *J. Geophys. Res.*, 114 (D18109).

Eckermann, S. D., 1995. On the observed morphology of gravity wave and equatorial-wave variance in the stratosphere, *J. Atmos. Terr. Phys.*, 57, 105-134.

Eckermann, S. D., Hirota, I., Hocking, W. K., 1994. Gravity wave and equatorial wave morphology of the stratosphere derived from long-term rocket soundings, *Q. J. R. Meteorol. Soc.*, 121, 149-186.

Ern, M., Preusse, P., Alexander, M. J., Warner, C. D., 2004. Absolute values of gravity wave momentum flux derived from satellite data, *J. Geophys. Res.*, 109, D20130, doi:10.1029/2004JD004752.

Forbes, J., 1995. Tidal and planetary waves, *Geoph. Monog. Series.*, 87, 67-87.

Fritts, D. C., Alexander, M. J., 2003. Gravity wave dynamics and effects in the middle atmosphere, *Rev. Geophys.*, 41(1), 1003, doi:10.1029/2001RG000106.

Fritts, D. C., Vincent, R. A., 1987. Mesospheric momentum flux studies at Adelaide, Australia: Observations and a gravity wave-tidal interaction model, *J. Atmos. Sci.*, 44, 605-619.

Fukao S., 2007. Recent advances in atmospheric radar study. *J. Meteorol. Soc. Jpn* 85B: 215–239.

Gong, J., Geller, M. A., Wang, L., 2008. Source spectra information derived from U.S. high-resolution radiosonde data, *J. Geophys. Res.*, 113, D10106, doi:10.1029/2007JD009252.

Graham, N. E., Diaz, H. F., 2001. Evidence for intensification of North Pacific winter cyclones since 1948, *Bull. Am. Meteorol. Soc.*, 82 (9), 1869–1893.

Hamilton, K., Vincent, R. A., 1995. High-resolution radiosonde data offer new prospects for research, *Eos*, 76 (49), doi:10.1029/95EO00308.

Hamilton, K., 1991. Climatological statistics of stratospheric inertia-gravity waves deduced from historical rocketsonde wind and temperature data, *J. Geophys. Res.*, 96, 20831-20829.

Hines, C. O., Tarasick, D. W., 1987. On the detection and utilization of waves in airglow studies, *Planet. Sp. Sci.*, 35(7), 851-866.

Hines, C. O., 1960. Internal atmospheric gravity waves at ionospheric heights, *Can. J. Phys.*, 38, 1441-1481.

Hirota, I., Niki, T., 1985. A statistical study of inertia-gravity waves in the middle atmosphere, *J. Meteorol. Soc. Jpn.*, 63, 1055-1066.

Holton, J. R., 2004. *An introduction to dynamic meteorology*. 4. Edition, Elsevier Academic Press, London.

Holton, J. R., 1983. The influence of gravity wave breaking on the general circulation of the middle atmosphere, *J. Atmos. Sci.*, 46, 2497-2507.

Höppner, K., Bittner, M., 2007. Evidence for solar signals in the mesopause temperature variability?, *J. Atmos. Sol. Terr. Phys.*, 69: 431–448.

Irvine, E. A., Gray, S. L., Methven, J., Renfrew, I. A., 2011. Forecast Impact of Targeted Observations: Sensitivity to Observation Error and Proximity to Steep Orography, *Mon. Weather Rev.*, 139, 69-78, doi:10.1175/2010MWR3459.1.

Jung, B.-J., Kim, H. M., Zhang, F., Wu, C.-C., 2011. Effect of targeted dropsonde observations and best track data on the track forecasts of Typhoon Sinlaku (2008) using an ensemble Kalman filter, *Tellus, A* (64), 14984, doi:10.3402/tellusa.v64i0.14984.

Karoly, D.J., Roff, G. L., Reede, M. J., 1996. Gravity wave activity associated with tropical convection detected in TOGA COARE sounding data, *Geophys. Res. Lett.*, 23 (3), 261-264.

Kim, Y.J., Arakawa, A., 1995. Improvement of orographic gravity wave parameterization using a mesoscale gravity wave model, *J. Atmos. Sci.*, 52, 1875-1902.

Kitamura, Y., Hirota, I., 1989. Small-scale disturbances in the lower stratosphere revealed by daily rawin sonde observations, *J. Meteorol. Soc. Jpn.*, 67, 817–830.

Kramer, R., Wüst, S., Schmidt, C., Bittner, M., 2015. Gravity wave characteristics in the middle atmosphere during the CESAR campaign at Palma de Mallorca in 2011/2012: Impact of extra-tropical cyclones and cold fronts, *J. Atmos. Sol. Terr. Phys.*, 128, 8-23, doi: 10.1016/j.jastp.2015.03.001.

Lehmann, C. I. , Kim, Y.-H. , Preusse, P., Chun, H.-Y., Ern, M., Kim, S.-Y., 2012. Consistency between Fourier transform and small-volume few-wave decomposition for spectral and spatial variability of gravity waves above a typhoon, *Atmos. Meas. Tech.*, 5, 1637–1651.

Li, T., Leblanc, T., McDermid, I., Wu, D., Dou, X., Wang, S., 2010 . Seasonal and interannual variability of gravity wave activity revealed by long-term lidar observations over Mauna Loa Observatory, Hawaii, *J. Geophys. Res.*, 115, D13103, doi:10.1029/2009JD013586.

Lindzen, R. S., Holton, J. R., 1968. A theory of the quasi-biennial oscillation, *J. Atmos. Sci.*, 25, 1095-1107.

Manzini, E., McFarlane, N. A., 1998. The effect of varying the source spectrum of a gravity wave parameterization in a middle atmosphere general circulation model, *J. Geophys. Res.*, 103, D24, 31523-31539.

McFarlane, N. A., 1987. The effect of orographically excited gravity wave drag on the general circulation of the lower stratosphere and troposphere, *J. Atmos. Sci.*, 44 (14), 1775-1800.

Mitchell, N. J., Thomas, L., Prichard, I. T., 1994. Gravity waves in the stratosphere and troposphere observed by lidar and MST radar, *J. Atmos. Terr. Phys.*, 56, 939-947.

Moffat-Griffin, T., Hibbins, R., Jarvis, M., Colwell, S., 2011. Seasonal variations of gravity wave activity in the lower stratosphere over an Antarctic Peninsula station, *J. Geophys. Res.*, 116, D14111, doi:10.1029/2010JD015349.

Nastrom, G. D., Fritts, D. C., Gage, K. S., 1987. An investigation of terrain effects on the mesoscale spectrum of atmospheric motions, *J. Atmos. Sci.*, 44, 3087-3096.

Orr, A., Bechtold, P., Scinocca, J., Ern, M., Janiskova, M., 2010. Improved middle atmosphere climate and forecasts in the ECMWF model through a non-orographic gravity wave drag parameterization, *J. Clim.*, 23, 5905-5926, doi:10.1175/2010JCLI3490.1.

Pfenninger, M., Ziu, A., Papen, G., Gardner, C., 1999. Gravity wave characteristics in the lower atmosphere at South Pole, *J. Geophys. Res.*, 104 (D6), 5963-5984.

Piani, C., Durran, D. R., Alexander, M. J., Holton, J. R., 2000. A numerical study of three-dimensional gravity waves triggered by deep convection and their role in the dynamics of the QBO, *J. Atmos. Sci.*, 57 (22), 3689-3702.

Plougonven, R., Zhang, F., 2014. Internal gravity waves from atmospheric jets and fronts, *Rev. Geophys.*, 52, doi:10.1002/2012RG000419.

Pulido, M., Polavarapu, S., Shepherd, T. G., Thuburn, J., 2012. Estimation of optimal gravity wave parameters for climate models using data assimilation, *Q. J. R. Meteorol. Soc.*, 138, 298-309.

Preusse, P., Dörnbrack, A., Eckermann, S. D., Riese, M., Schaefer, B., Bacmeister, J. T., Broutman, D., Grossmann, K. U., 2002. Space-based measurements of stratospheric mountain waves by CRISTA. 1. Sensitivity, analysis method, and a case study, *J. Geophys. Res.*, 107, 8178, doi:10.1029/2001JD000699.

Riggin, D. M., Fritts, D. C., Fawcett, C. D., Kudeki, E., Hitchman, M. H., 1997. Radar observations of gravity waves over Jicamarca, Peru during the CADRE campaign, *J. Geophys. Res.*, 102, 26263-26281.

Sato, K., O'Sullivan, D., Dunkerton, T. J., 1997. Low-frequency inertia-gravity waves in the stratosphere revealed by three-week continuous observation with the MU radar, *Geophys. Res. Lett.*, 24, 1739-1742.

Sato, K., 1994. A statistical study of the structure, saturation and sources of inertia-gravity waves in the lower stratosphere observed with the MU radar, *J. Atmos. Terr. Phys.*, 56, 755-774.

Schmidt, C., Höppner, K., Bittner, M., 2013. A ground-based spectrometer equipped with an InGaAs array for routine observations of OH(3-1) rotational temperatures in the mesopause region located at the NDMC-station Oberpfaffenhofen, Germany, *J. Atmos. Terr. Phys.*, 102, 125-139, doi:10.1016/j.jastp.2013.05.001.

Schneider, R. S., 1990. Large-Amplitude mesoscale wave disturbances within intense Midwest extratropical cyclone of 15 December 1987, *Weath. Forecasting*, 5 (4), 533-558.

Song, I.-S., Chun, H.-Y., 2005. Momentum Flux Spectrum of Convectively Forced Internal Gravity Waves and Its Application to Gravity Wave Drag Parameterization. Part I: Theory, *J. Atmos. Sci.*, 62, 107-124.

Stevens, B., Giorgetta, M., Esch, M., Mauritsen, T., Crueger, T., Rast, S., Salzmann, M., Schmidt, H., Bader, J., Block, K., Brokopf, R., Fast, I., Kinne, S., Kornbluh, L., Lohmann, U., Pincus, R., Reichler, T., Roeckner, E., 2013. Atmospheric component of the MPI-M Earth System Model: ECHAM6, *J. Adv. Model. Earth Syst.*, 5, 1-27, doi:10.1002/jame.20015.

Swenson, G. R., M. J. Alexander, Haque, R., 2000. Dispersion imposed limits on atmospheric gravity waves in the mesosphere: observations from OH airglow, *Geophys. Res. Lett.*, 27(6), 875-878.

Thompson, D. W. J., D. J. Seidel, W. J. Randel, C.-Z. Zou, A. H. Butler, C. Mears, A. Osso, C. Long and R. Lin, 2012. The mystery of recent stratospheric temperature trends, *Nature Perspective Research*, Vol. 491(695), doi:10.1038/nature11579.

Ulbrich, U., Pinto, J. G., Kupfer, H., Leckebusch, G. C., Spanghel, T., Reyers, M., 2007. Changing northern hemisphere storm tracks in an Ensemble of IPCC climate change simulations. *J. Clim.*, 21, 1669–1679.

Vincent, R. A., S. J. Allen, Eckermann, S. D., 1997. Gravity-wave parameters in the lower stratosphere, *Gravity Wave Processes: Their Parameterization in Global Climate Models*, NATO ASI Ser. I, 50, edited by K. Hamilton, pp. 7-25, Springer-Verlag.

Wang, L., Geller, M. A., 2003. Morphology of gravity-wave energy as observed from 4 years (1998-2001) of high vertical resolution U.S. radiosonde data, *J. Geophys. Res.*, 108 (D16), 4489, doi:10.1029/2002JD002786.

Wüst, S., Bittner, M., 2008. Gravity wave reflection: Case study based on rocket data, *J. Atmos. Sol. Terr. Phys.*, 70, 742–755.

Wüst, S., Bittner, M., 2006. Non-linear resonant wave–wave interaction (triad): Case studies based on rocket data and first application to satellite data, *J. Atmos. Sol. Terr. Phys.*, 68, 959–976, doi:10.1016/j.jastp.2005.11.011.

Yoshiki, M., Sato, K., 2000. A statistical study of gravity waves in the Polar regions based on operational radiosonde data, *J. Geophys. Res.*, 105, 17995-18011.

Zhang, S. D., Huang, C. M., Huang, K. M., Yi, F., Zhang, Y. H., Gong, Y., Gan, Q., 2014. Spatial and seasonal variability of medium- and high-frequency gravity waves in the lower atmosphere revealed by US radiosonde data, *Ann. Geophys.*, 32, 1129-1143, doi: 10.5194/angeo-32-1129-2014.

Zhang, S., Yi, F., Huang, C., Huang, K., 2012. High vertical resolution analyses of gravity waves and turbulence at a midlatitude station, *J. Geophys. Res.*, 117, D02103, doi:10.1029/2011JD016587.

Fig 1: Times series of maximum altitudes from radiosonde measurements at Prague during 1997-2009. Solid line denotes the 25 km minimum altitude limit used for analyses.

Figure 1

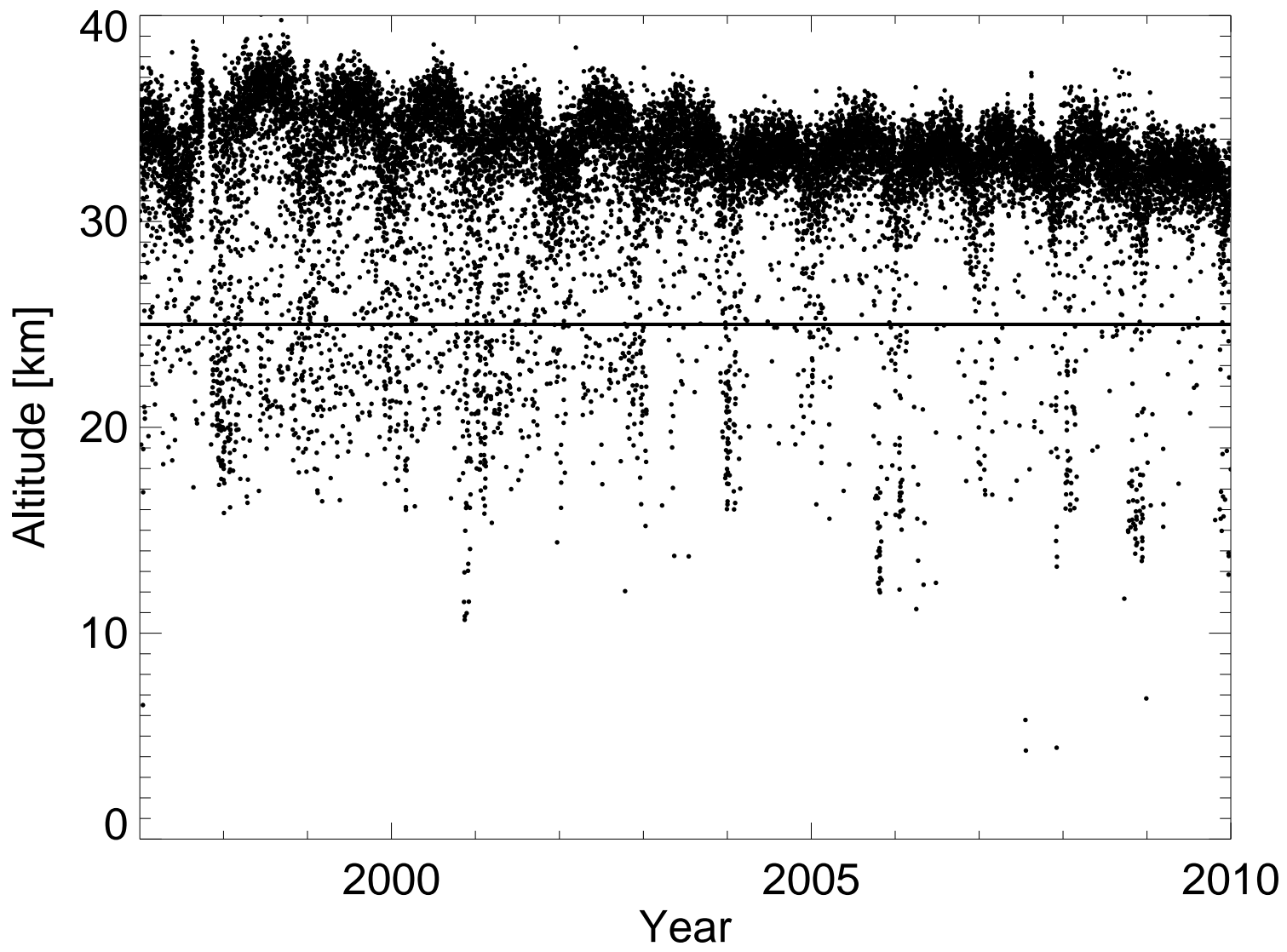


Fig 2: Example for the superposition principle: Temperature profile (solid line) and background temperature (dashed line) as well as the resulting temperature perturbations (dash-dot line) for the 1st December 2009, 0 UTC.

Figure 2

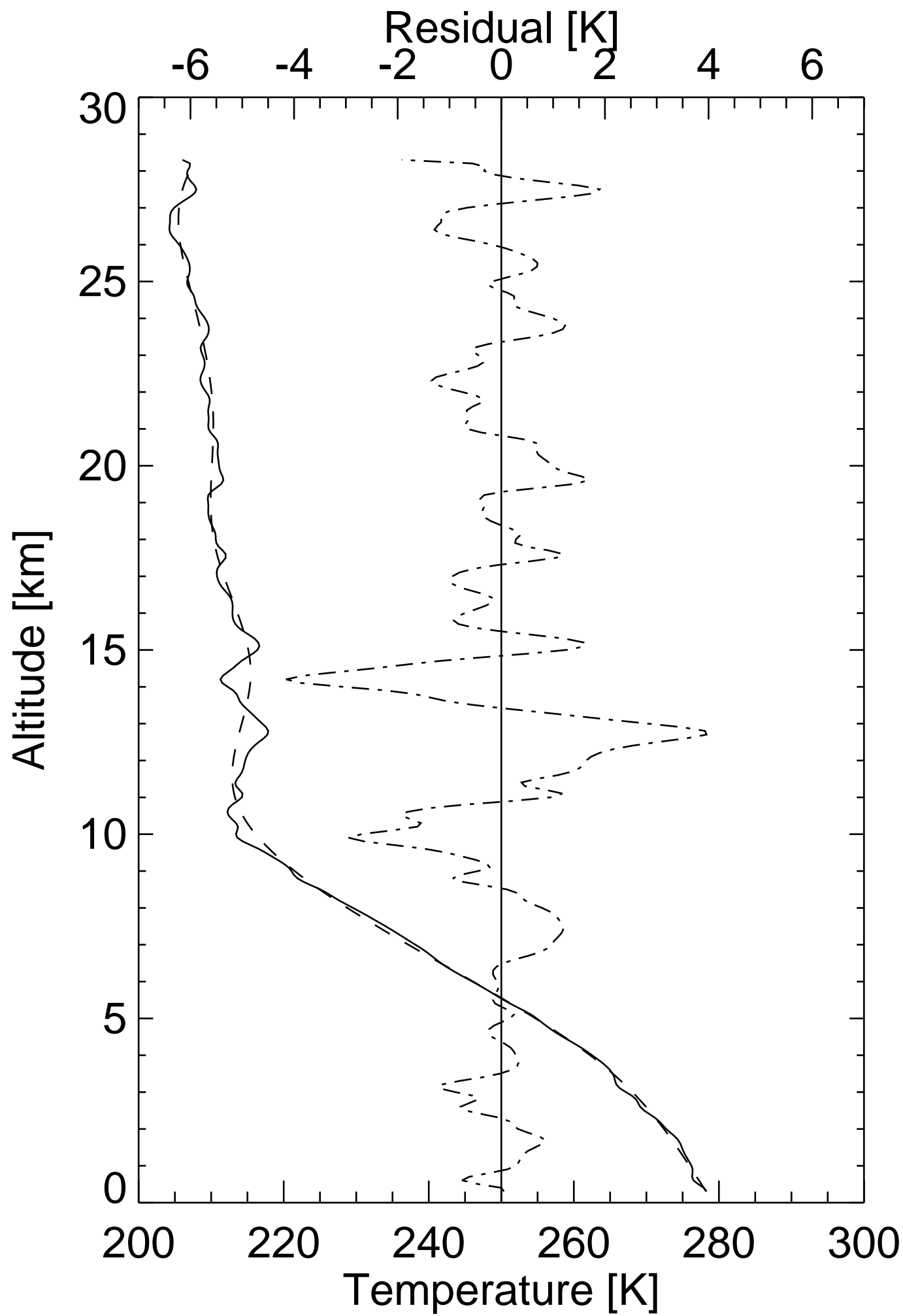


Figure caption 3

Fig 3: Normalized gravity wave activity for three different altitude ranges: 17-25 km (a), 15-28 km (b), 15-30 km (c), exemplarily shown for year 1998. All three time series show the same strong GW signatures, especially during winter time.

Figure 3

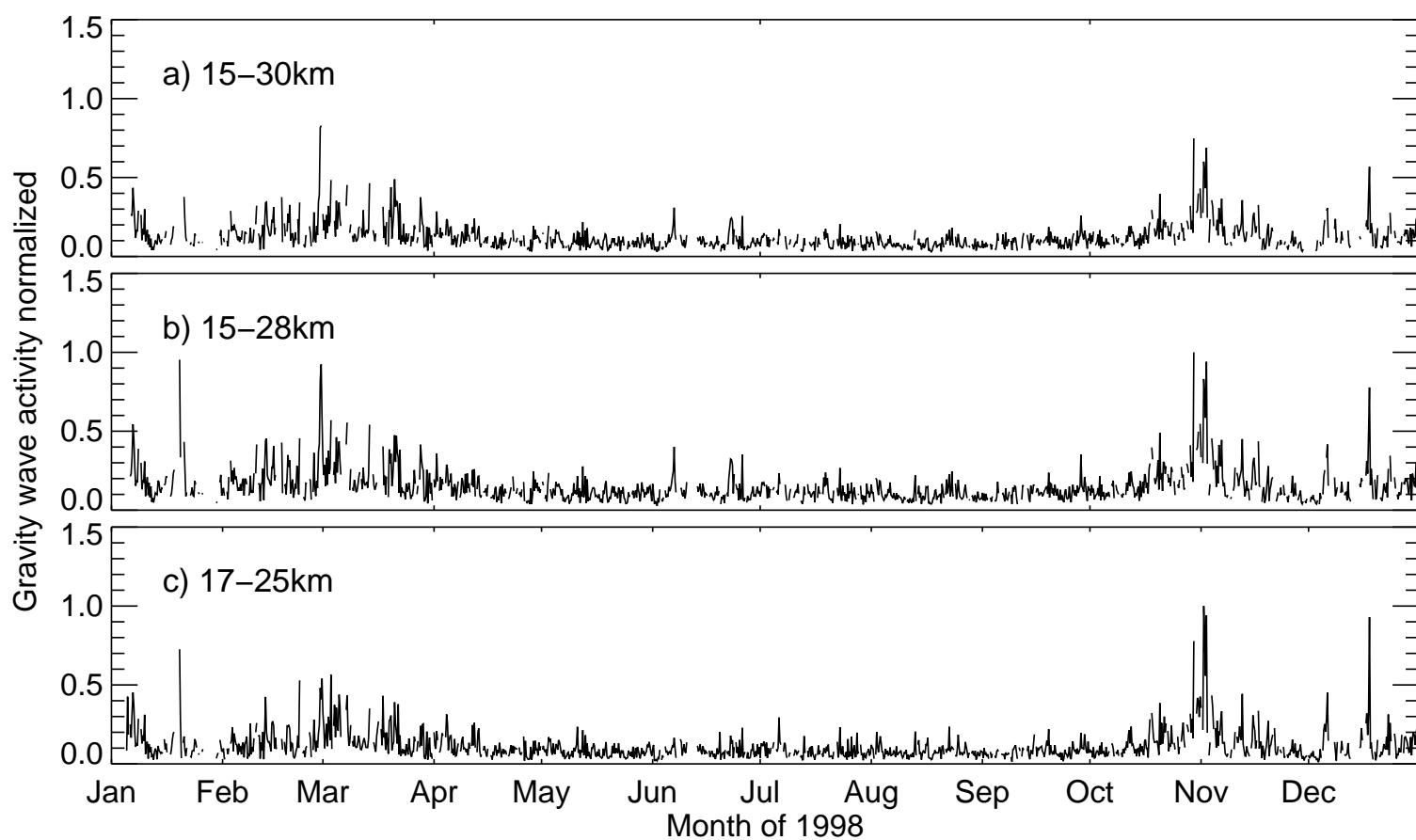


Fig 4: Gravity wave activity for the lower stratosphere (17-25 km) shown for the years 2003-2005 (black solid line) with the corresponding surface pressure at Prague in hPa (dashed line). Red boxes denote winter time, whereas black boxes mark periods with enhanced corresponding low surface pressure and peak gravity wave activity.

Figure 4

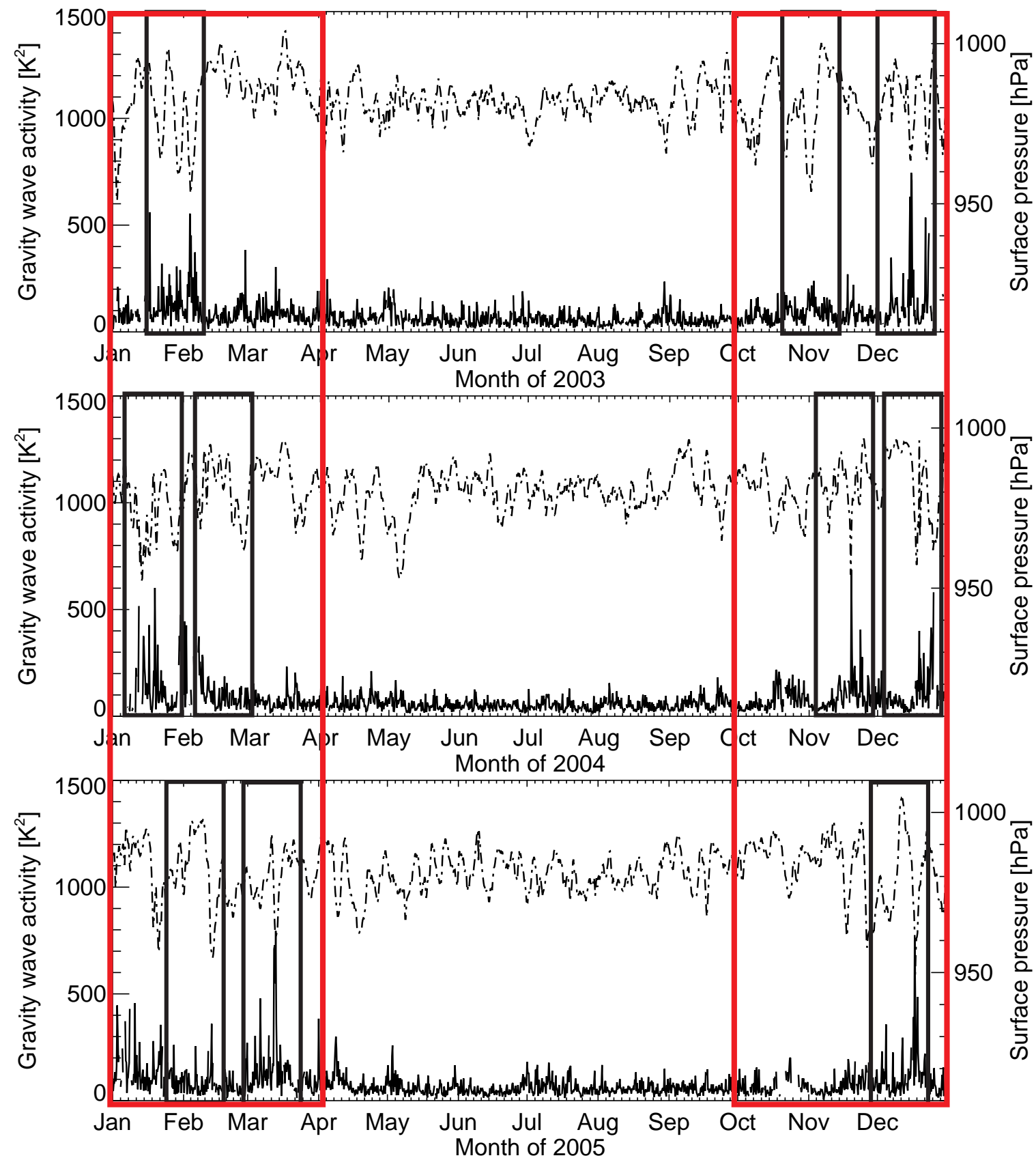


Fig 5: Mean stratospheric gravity wave activity for the whole measurements period (1997-2009) in K^2 . The black horizontal line marks the absolute average of the whole GWA time series. The grey solid line denotes the three main periods of the annual variation: ~ 1 year, $\sim 1/2$ year and $\sim 1/3$ year, which are calculated by harmonic analysis. Dashed vertical lines denote more or less the transitions of winter to summer period and vice versa.

Figure 5

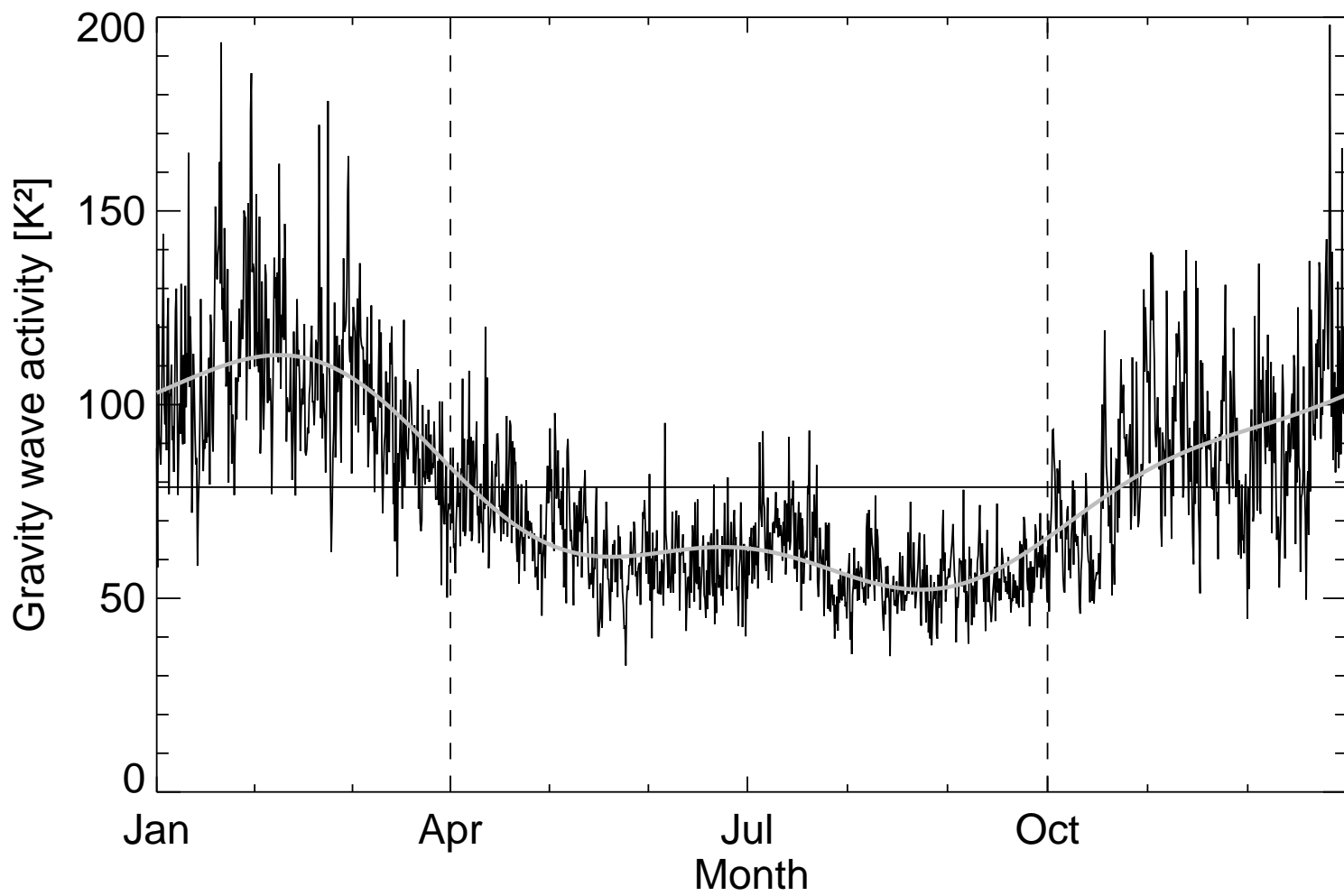


Fig 6: Gravity wave activity (upper part) combined with negative surface pressure gradient within 12 hours ($\Delta p = p_2 - p_1$, whereby Δp is correlated to GWA_2 ; lower part) for January to March 1997. Gray solid lines are hand drawn and included to guide the eye.

Figure 6

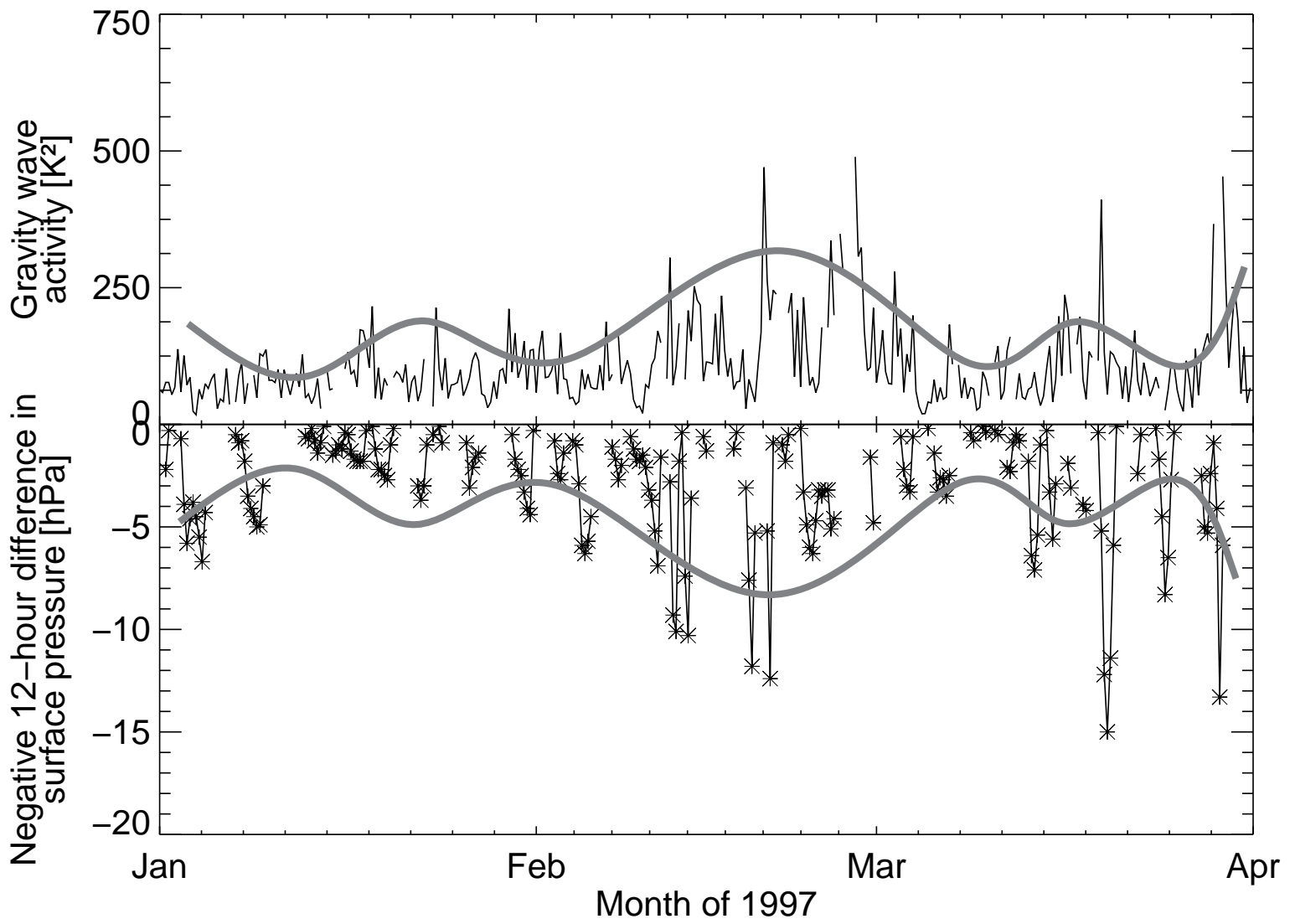


Fig 7: Vertical momentum flux for the zonal and meridional component with error bars (gray), respectively integrated for the stratospheric altitude regime between 17 and 25 km altitude (black solid line) in 1999. Surface pressure at Prague (dashed line) is also shown.

Figure 7

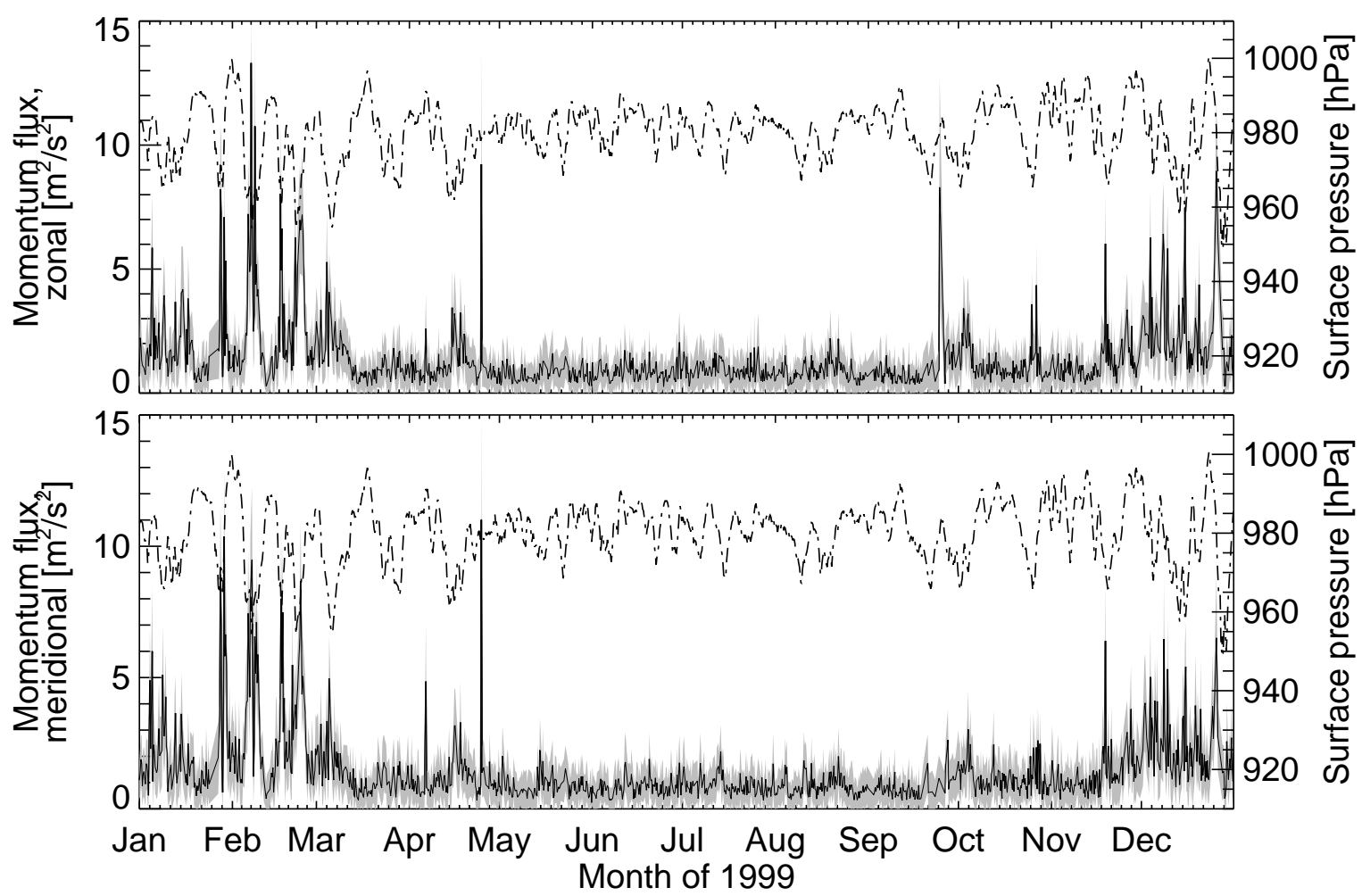


Fig 8: Time series of momentum flux fluctuations (a) and ground pressure fluctuations (b) between 01.01.1997 and 31.03.1997 with corresponding wavelet relative intensities. Upper wavelet contour plot shows the periods between 12 and 600 hours, the lower one focuses on periods from 12 to 240 hours (also marked with the black rectangle in the upper wavelet plot). White lines denote the 95% significance limit.

Figure 8a

a)

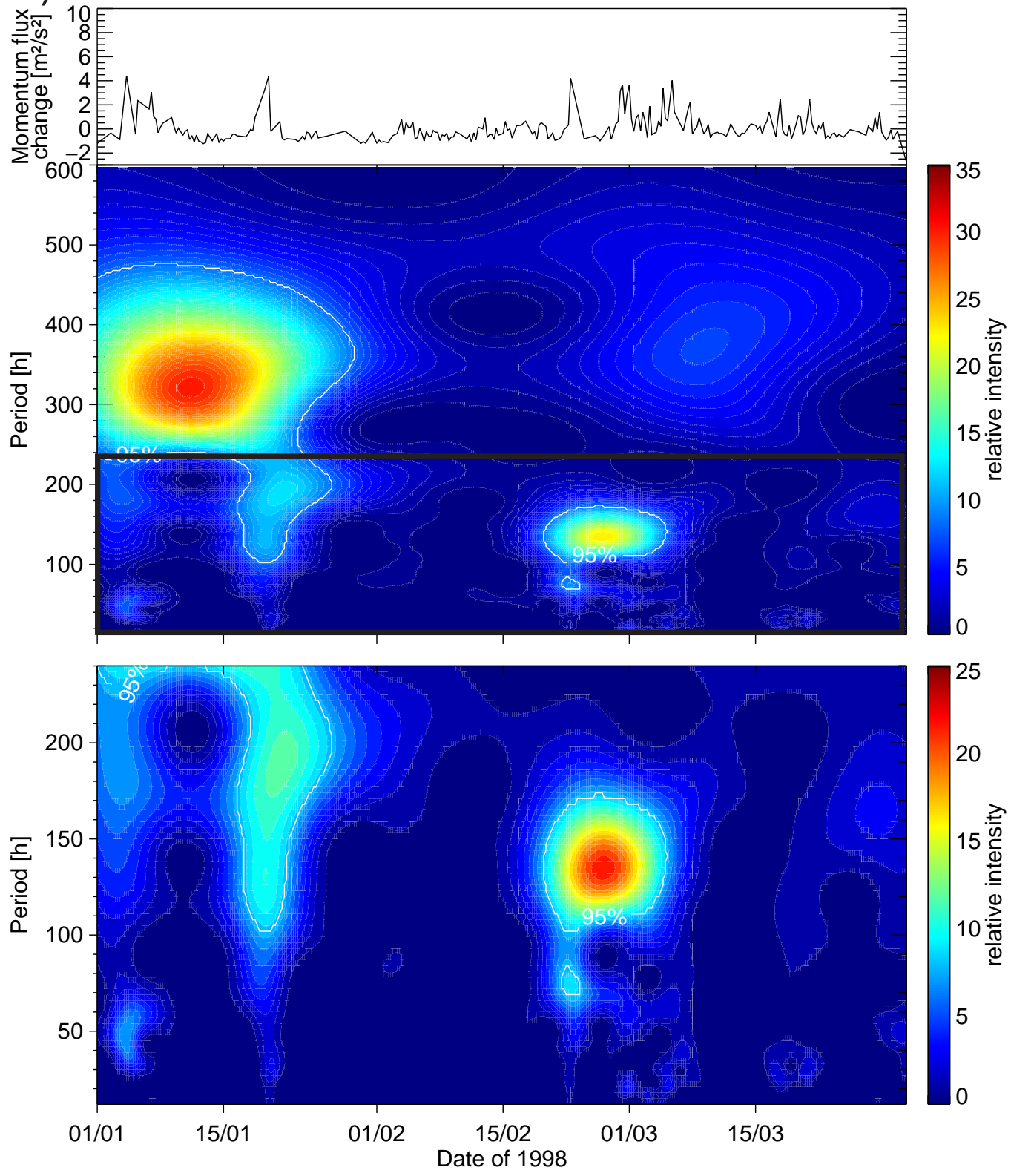


Figure 8b

b)

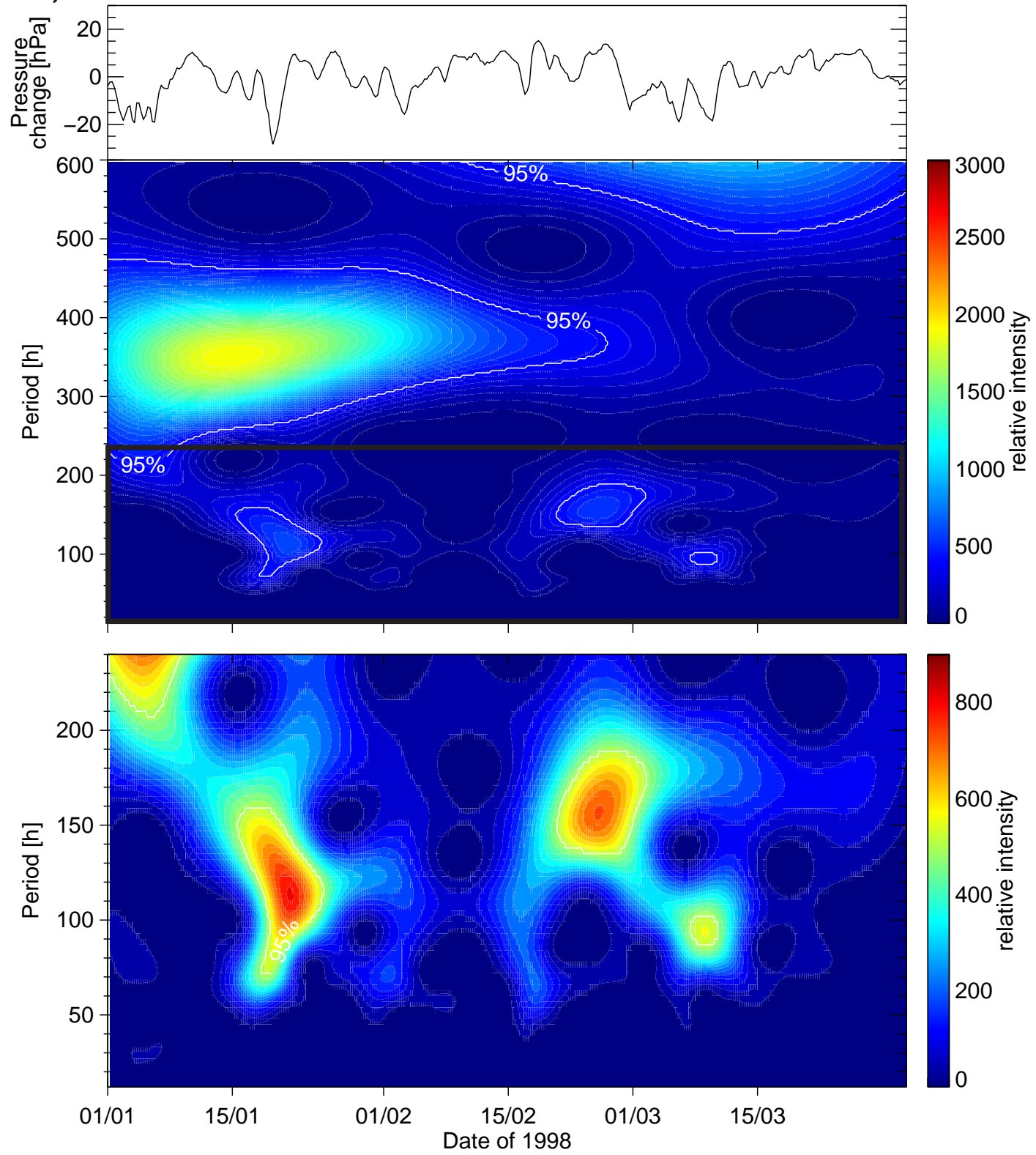


Fig A1: Mean uncertainty of the detrending method for temperature (left) and wind speed (right) depending on altitude (black solid lines). Dashed space marks the uncertainty range of the radiosonde sensors for temperature (0.5 K) and wind speed (0.7 m/s) itself.

Figure A1

